Midlevel Vorticity Structure of the 10–11 June 1985 Squall Line

M. I. BIGGERSTAFF AND R. A. HOUZE, JR.

Department of Atmospheric Sciences, University of Washington, Seattle, Washington

(Manuscript received 8 November 1990, in final form 1 May 1991)

ABSTRACT

The comprehensive analysis of the kinematic structure of the mature phase of the 10–11 June 1985 squall-line system was used to examine the midlevel vertical-vorticity structure of the storm to show that relative vertical vorticity in the stratiform region at midlevels was organized into bands (both cyclonic and anticyclonic) oriented parallel to the convective line, with anticyclonic vorticity between the rear of the convective line and the heaviest stratiform precipitation and cyclonic vorticity farther back. Since previous studies have not found anticyclonic vorticity over such a large portion of the stratiform region at midlevels and since the concentration of anticyclonic vorticity may have been detrimental to the longevity of the storm by limiting the development of an inertially stable cyclonic circulation, the tilting and stretching terms of the vertical-vorticity equation were computed to determine how the observed vertical-vorticity pattern was maintained. Tilting of horizontal vorticity into vertical vorticity by gradients of vertical motion was a factor of 2–10 greater than the stretching of vertical vorticity. Below the melting level and at the rear of the stratiform region, tilting was associated with gradients of mesoscale vertical motion. Above the melting level, near the convective line, tilting was associated with gradients of mean convective motions.

1. Introduction

The precipitation and kinematic structure of the mature phase of the 10–11 June 1985 squall line observed during the Preliminary Regional Experiment for Stormscale Operational Research Meteorology—Central Phase (Cunning 1986) was examined using a comprehensive analysis that combined high-frequency rawinsonde, profiler, surface mesonet, and dual-Doppler data in a common framework attached to the moving storm (Biggerstaff and Houze 1991, hereafter referred to as BH). Figure 1 is a schematic showing the midlevel vertical-vorticity structure of the stratiform region of the 10–11 June 1985 squall line based on the kinematic structure presented in BH. Bands of positive and negative vertical vorticity, oriented parallel to the convective line, were found in the stratiform region at midlevels with negative vorticity between the rear of the convective region and the area of heaviest stratiform precipitation and positive vorticity farther back.

Previous studies have shown that positive vorticity is often observed at midlevels in the stratiform region of squall-line systems (Houze 1977; Ogura and Liou 1980; Gamache and Houze 1982, 1985; Leary and Rappaport 1987). Numerical simulations of mesoscale convective systems (MCSs) indicate that positive vorticity may result from geostrophic adjustment of the air at midlevels in response to a mesolow that occurs beneath the warm trailing anvil cloud (Zhang and Fritsch 1987, 1988b). The stretching that occurs in association with convergence into the mesolow amplifies the ambient absolute vorticity, which tends to be positive. Occasionally, the midlevel positive vorticity develops into a deep cyclonic mesovortex that dominates the circulation within the stratiform region and alters the distribution of precipitation behind the convective line (Houze et al. 1989; Brandes 1990). Such mesovortices may also become inertially stable and increase the longevity of the MCS (Zhang and Fritsch 1987).

Although the structure and importance of midlevel positive vorticity in the stratiform region of squall-line systems has been clearly documented by earlier studies, no previous study has documented the structure and importance of the midlevel negative vorticity shown in Fig. 1. Indeed, previous observational studies have not found negative vorticity between the convective line and the heaviest stratiform precipitation of squall-line systems. However, a model simulation of the 10–11 June 1985 storm produced anticyclonic vorticity in association with the mesoscale downdraft behind the convective line (Zhang et al. 1989, hereafter referred to as ZGP). Either the midlevel vertical-vorticity structure of the 10–11 June 1985 storm was unique or, because of poor horizontal resolution in studies lacking Doppler radar coverage (Houze 1977; Ogura and Liou 1980; Gamache and Houze 1982, 1985; Leary and Rappaport 1987) and limited aerial coverage in studies with Doppler radar data (Heymsfield and

Corresponding author address: Dr. Michael I. Biggerstaff, Department of Meteorology, College of Geosciences, Texas A&M University, College Station, TX 77843.

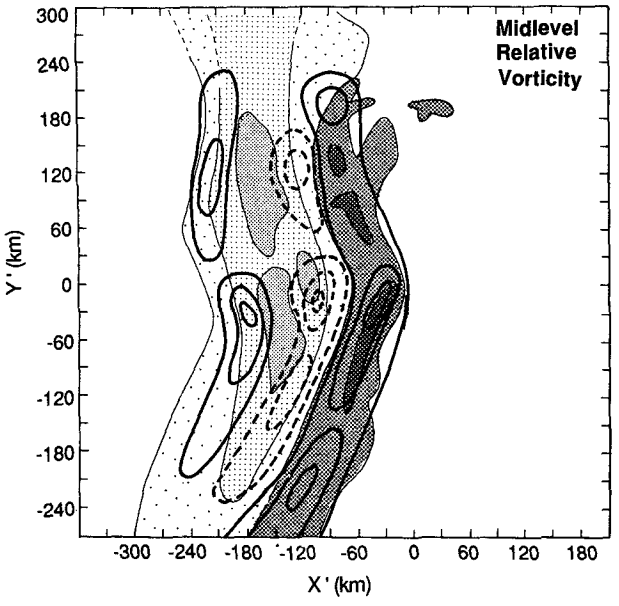

FIG. 1. Schematic of a plan view of the midlevel relative vertical-vorticity structure of the 10–11 June 1985 squall-line system. Solid (dashed) contours indicate positive (negative) vorticity. Contours in the convective region are at twice the interval used in the stratiform region.

Schotz 1985; Smull and Houze 1987; Srivastava et al. 1986; Kessinger et al. 1987; Chong et al. 1987; Roux 1988), the previous studies were incapable of resolving the anticyclonic part of the circulation within the stratiform region of other squall-line systems.

A region of anticyclonic vorticity associated with a meso-β-scale[1] vortex couplet observed in a small cluster of weak multicellular convection over Kansas was recently documented by Verlinde and Cotton (1990). The vorticity couplet they observed, centered near the convective region of the nonsquall system, had a cyclonic circulation of radius $\sim$ 15 km in the trailing anvil region and an anticyclonic circulation of radius $\sim$ 10 km near the forward anvil region. Thus, the vorticity pattern they observed was unlike the pattern shown in Fig. 1 for the stratiform region of the 10–11 June 1985 storm; moreover, the role of the anticyclonic part of the vortex couplet in the evolution of the small multicellular convective cluster was not discussed.

The objective of this paper is to document the seemingly unique structure of the banded midlevel vertical-vorticity pattern observed in the stratiform region of the 10–11 June 1985 storm and to examine how that vorticity pattern may have developed. Specifically, the comprehensive combined analysis of Doppler radar, sounding, profiler, and surface mesonet data constructed by BH is used to show that tilting of across-line horizontal vorticity by the mesoscale vertical motion in the stratiform region at midlevels was sufficient to maintain the bands, oriented parallel to the convective line, of positive and negative vertical vorticity in the stratiform region. The band of anticyclonic vorticity may have been detrimental to the longevity of the storm system by limiting the development of an inertially stable cyclonic circulation.

[1] Meso-β-scale, in the terminology of Orlanski (1975), refers to horizontal scales from 20 to 200 km.

2. Data and method of analysis

In this study, the three-dimensional relative winds from BH that were digitized at 15-km intervals over a 570-km × 570-km horizontal grid for the 150, 200, 300, 400, 500, 550, 600, 675, 800, and 900 mb and surface levels are used to determine the midlevel horizontal and vertical-vorticity structure of the squall-line system. In isobaric coordinates the vorticity vector, defined as the curl of the wind field, can be written as:

$$\omega = \left(\rho g \frac{\partial v}{\partial p} - \frac{1}{\rho g}\frac{\partial \omega}{\partial y}\right)\mathbf{i} + \left(\frac{1}{\rho g}\frac{\partial \omega}{\partial x} - \rho g \frac{\partial u}{\partial p}\right)\mathbf{j} + \left(\frac{\partial v}{\partial x} - \frac{\partial u}{\partial y}\right)\mathbf{k} \quad (1)$$

or

$$\omega = \omega_H + \zeta \mathbf{k}, \quad (2)$$

where ω_H is the horizontal-vorticity vector, ζ the relative vertical vorticity, ρ the density determined from the rawinsonde data, g the gravitational acceleration, and u, v, ω the zonal, meridional, and vertical components of motion, respectively. In (1) it has been assumed that ω can be approximated by $-\rho g w$ where w is the geometric vertical motion (see Holton 1979).

In the comprehensive composite study of BH, high-frequency rawinsonde, profiler, surface mesonet, conventional radar, and Doppler radar data collected during the 10–11 June 1985 storm were used to examine the precipitation and kinematic structure of the mature phase of the squall-line system. The reader is referred to BH for a thorough discussion of the data comprising the composite analysis and how those data were placed in a coordinate system attached to the moving storm (i.e., the composite coordinate system). Here we note that the orientation of the axes of the composite coordinate system was determined by defining the positive X' axis to be in the direction of the storm-motion vector (18 m s^{-1} toward 125°). As a result, north is 35° counterclockwise from the positive Y' axis. For simplicity, the half of the squall line extending into the region of positive Y' will be referred to as the "northern" portion of the line, with the remainder referred to as the "southern" portion of the line.

Figure 2 shows the composite low-level radar reflec-

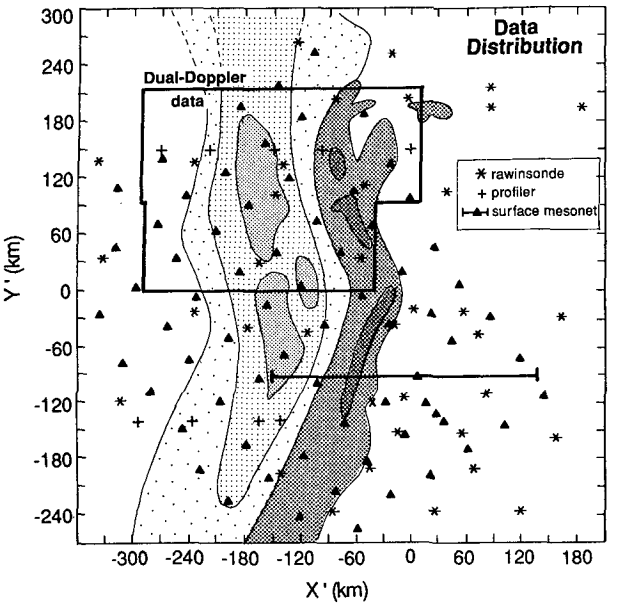

FIG. 2. Distribution of data relative to the composite radar reflectivity pattern. The X' axis points toward 125° from north.

tivity structure of the squall line as determined by BH and illustrates the reference frame used in this paper. In the composite framework, the convective line was roughly 60 km wide and followed by a region of stratiform precipitation that was approximately 150 km wide. Stratiform precipitation was also found to the north of the convective line. An area of enhanced reflectivity (the secondary band) was found within the stratiform region at a fairly constant distance from the rear of the convective line, but it was widest and best defined in the northern portion of the squall-line system. As shown by BH, the strongest portions of reflectivity within the secondary band, associated with the heaviest stratiform precipitation, were located downwind of the enhanced regions of reflectivity within the convective line.

The locations of rawinsonde, profiler, surface mesonet data, and the region covered by dual-Doppler analyses in the composite coordinate system from which the kinematic structure of the 10–11 June 1985 storm was determined are also shown in Fig. 2. As indicated, the presquall environment was well sampled by rawinsondes. A reasonable number of rawinsondes also sampled the postsquall environment and the precipitating portions of the MCS. Many of the rawinsondes released in the stratiform region, however, did not survive above the melting level; consequently, the distribution of data points at upper levels was not as good as that in Fig. 2. Fortunately, the profiler data provided excellent vertical cross sections of horizontal winds through the stratiform and postsquall regions. Moreover, the dual-Doppler analyses provided high-resolution coverage over the entire breadth of the northern half of the convective system. Thus, the northern portion of the convective system was extremely well sampled while the southern portion of the convective system was sampled somewhat less intensively, especially at upper levels.

3. Midlevel vertical-vorticity structure of the trailing stratiform region

a. Observed structure

The 10–11 June 1985 storm did not exhibit a dominant cyclonic vertical-vorticity structure at midlevels in the trailing stratiform region. Instead, cyclonic and anticyclonic vorticity apparently organized into bands oriented nearly parallel to the convective line (Fig. 3). A band of anticyclonic relative vorticity was located between the rear of the convective region and the enhanced portions of the secondary band. Farther back was a band of cyclonic vorticity. This banded vorticity pattern was evident over most of the stratiform region from about 500 to 800 mb. At midlevels just below the melting layer[2] (Fig. 3b), the banded vorticity structure was best established in the southern portion of the stratiform region. Closer to the surface (Fig. 3c), the pattern was still prevalent but the magnitudes of vertical vorticity, especially those associated with the cyclonic vorticity band, were not as strong, resulting in a weaker overall vorticity pattern. Above the melting layer (e.g., Fig. 3a), the banded vorticity pattern was most evident in the northern portion of the stratiform region where data coverage was best. Little anticyclonic vorticity was found above the melting level in the southern portion of the stratiform region where data coverage was relatively sparse.

Smaller-scale cyclonic and anticyclonic circulations were associated with the bands of vertical vorticity, especially near the melting level. A weak cyclonic mesovortex associated with the larger-scale band of cyclonic vorticity was observed from 650 to 750 mb in the relative flow just to the rear of the heaviest stratiform precipitation in the central portion of the squall-line system (see region near $X' = -180$, $Y' = 0$ in Fig. 13a of BH). As evidenced by the broad rear-to-front relative flow in which the weak cyclonic mesovortex was embedded, the cyclonic mesovortex did not dominate the circulation in the stratiform region. Moreover, an anticyclonic circulation, associated with the larger-scale band of anticyclonic vorticity, was also observed from 600 to 700 mb in the trailing stratiform region of the 10–11 June 1985 storm, but it was closer to the convective line (e.g., near $X' = -150$, $Y' = 110$ at 675 mb in Fig. 13a of BH).

The band of anticyclonic vertical vorticity, with its associated small-scale anticyclonic mesovortex, is a part

[2] The melting layer was near 625 mb in the stratiform region of the 10–11 June 1985 storm.

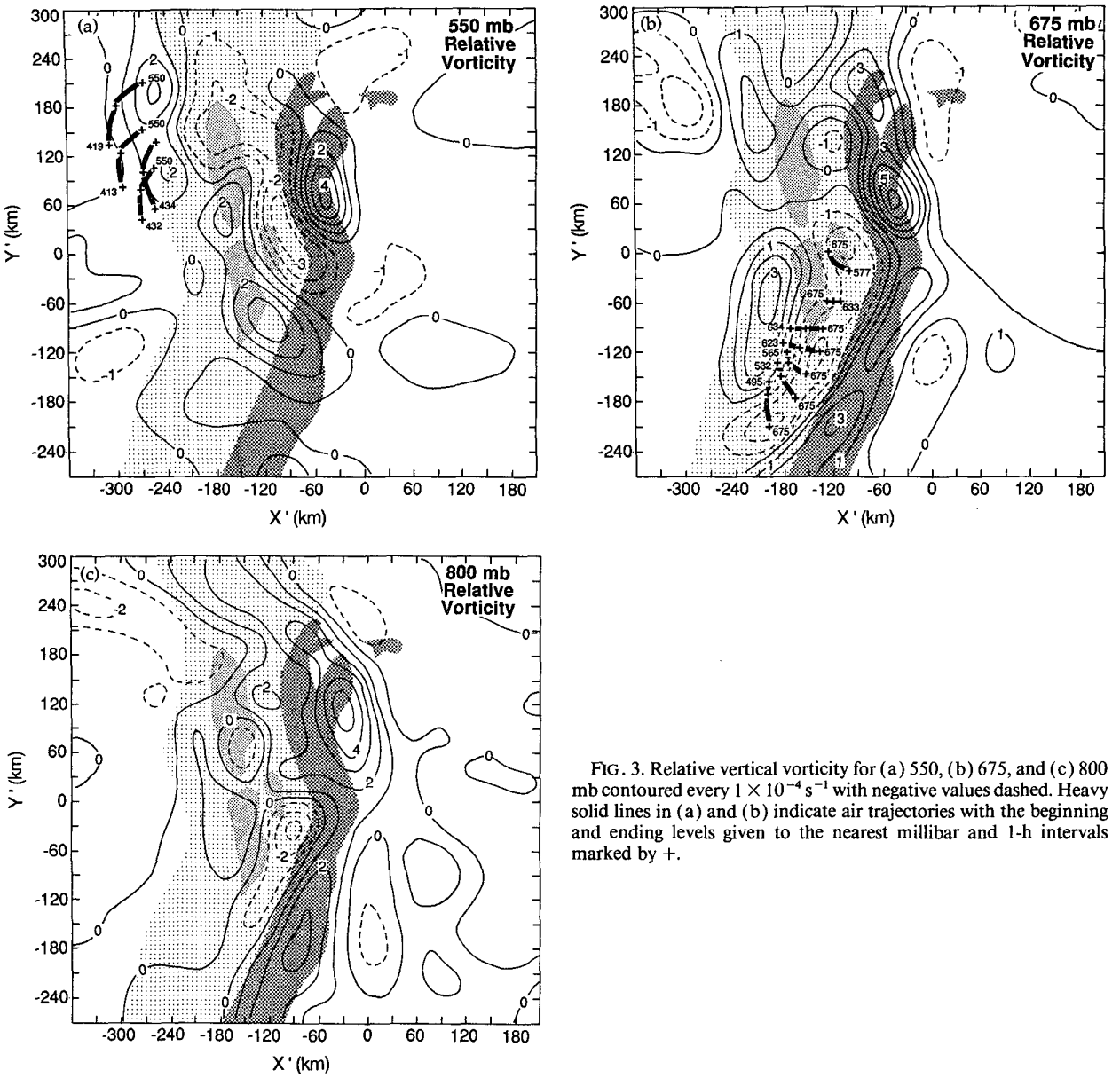

FIG. 3. Relative vertical vorticity for (a) 550, (b) 675, and (c) 800 mb contoured every 1×10^{-4} s^{-1} with negative values dashed. Heavy solid lines in (a) and (b) indicate air trajectories with the beginning and ending levels given to the nearest millibar and 1-h intervals marked by +.

of the circulation within squall-line systems that has been hitherto undocumented. Previous studies have indicated that *cyclonic* vorticity is *often* observed at midlevels in the stratiform region of squall-line systems (Houze 1977; Ogura and Liou 1980; Gamache and Houze 1982, 1985; Leary and Rappaport 1987; Houze et al. 1989; Brandes 1990). Close examination of the previous studies indicate that the cyclonic vorticity was centered just *behind* the heaviest stratiform precipitation (see Figs. 5 and 15 in Houze 1977; Figs. 6 and 18 in Ogura and Liou 1980; Figs. 4 and 7 in Gamache and Houze 1982; Figs. 28 and 32 in Leary and Rappaport 1987; Fig. 5 in Houze et al. 1989; Fig. 15 in Brandes 1990). Thus, the band of cyclonic vorticity with its associated cyclonic mesovortex observed behind the heaviest stratiform precipitation in the 10–11 June 1985 storm appears to be a common feature among squall-line systems. In contrast, none of the aforementioned studies have documented the band of anticyclonic vorticity between the convective region and the heaviest stratiform precipitation.

The organization of vertical vorticity into bands oriented parallel to the convective line may have been an impediment to maintaining, or developing, a steady mesoscale circulation within the storm system. In particular, an inertially stable cyclonic circulation, which is thought to be a characteristic of long-lived MCSs (Zhang and Fritsch 1987), would not have been able

to develop at midlevels in the stratiform region where anticyclonic vorticity was being concentrated. In fact, the anticyclonic vorticity was apparently strong enough to create regions of negative absolute vorticity, associated with inertial *instability,* throughout large portions of the stratiform precipitation region. Consistent with the lack of an inertially stable cyclonic vortex, the 10–11 June 1985 storm was not extremely long lived. Since the midlevel band of anticyclonic vorticity in the stratiform region may have impaired the longevity of the storm system, it is important to try to determine how this band of anticyclonic vorticity was organized and maintained.

b. Simulated vertical-vorticity structure

The observed vertical vorticity at 675 and 800 mb (Figs. 3b and 3c, respectively) is similar to that obtained at 850 mb in the ZGP simulation of the 10–11 June 1985 storm (Fig. 4). The simulated storm had strong cyclonic vorticity in the northern portion of the convective line with moderate cyclonic vorticity extending throughout the rest of the convective region. Just to the rear of the convective line, a band of anticyclonic vorticity, with the strongest anticyclonic vorticity near the central portion of the system, extended southward parallel to the convective line. Little anticyclonic vorticity was present in the northern portion of the simulated stratiform region at 850 mb. A band of cyclonic vorticity was found along the back edge of the simulated stratiform region with a separate center to the rear of the strongest anticyclonic vorticity. Evidently, the detailed structure of the vertical vorticity observed in the stratiform region of the 10–11 June 1985 storm was well reproduced in the storm simulation.

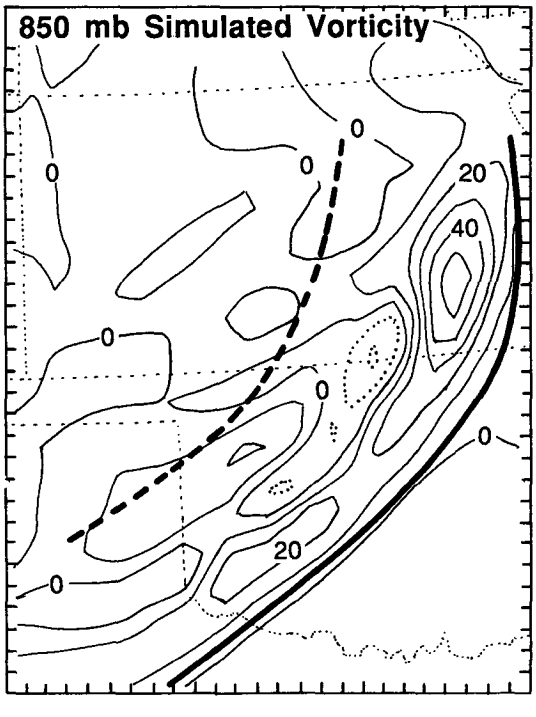

FIG. 4. The 850-mb relative vertical vorticity for the simulated 10–11 June 1985 storm, from Zhang et al. (1989). The heavy solid (dashed) line indicates the approximate location of the leading (trailing) edge of the squall-line system. Units are 10^{-4} s^{-1} with negative values dashed.

ZGP note that the anticyclonic vorticity was associated with mesoscale downdrafts and that the anticyclonic vorticity was controlled by the distribution of divergence and convergence. They do not, however, give a detailed description of how the simulated vertical-vorticity pattern developed. The comprehensive composite analysis presented in BH will be used to address how the banded vertical-vorticity structure in the stratiform region was maintained. Since the storm was assumed to be steady in the composite framework, the comprehensive analysis cannot be used explicitly to show how the vertical-vorticity structure developed. Nonetheless, the physical processes that maintained the observed vertical-vorticity structure were probably dominant during its development.

4. Importance of tilting and stretching

a. The vertical-vorticity equation

Using the same approximations as in (1), the equation describing the time rate of change of vertical vorticity following a parcel in isobaric coordinates for a frictionless atmosphere on a constant f plane is

$$\frac{D\zeta}{Dt} = (\zeta + f)\frac{\partial \omega}{\partial p} + \omega_H \cdot \nabla\left(\frac{-\omega}{\rho g}\right), \qquad (3)$$

where f is the Coriolis parameter and all other symbols are as defined in (1) and (2). The first term of the right-hand side of (3) is the "stretching," which acts to increase the magnitude of absolute vorticity $(\zeta + f)$ when vertical vortex tubes are stretched $(\partial\omega/\partial p > 0)$ and decrease the magnitude of absolute vorticity when vortex tubes are compressed $(\partial\omega/\partial p < 0)$. By itself, stretching cannot change the sign of a parcel's absolute vorticity. The second term on the right-hand side of (3) represents the "tilting" of horizontal vorticity into the vertical by a nonuniform vertical-motion field. Tilting can change the sign of a parcel's absolute vertical vorticity. Both terms have been evaluated for the 10–11 June 1985 storm.

To aid in visualizing the results, the magnitude and direction of ω_H, the horizontal-vorticity vector, are shown by means of streamlines and isotachs (e.g., Fig. 5a). Thus, the circulation implied by ω_H can be determined by the "right-hand rule" where the right-hand thumb points in the direction of the vorticity vector, and the curled fingers of the right hand represent the direction of the circulation. The scalar fields of tilting of ω_H and stretching of $(\zeta + f)$ are illustrated by means

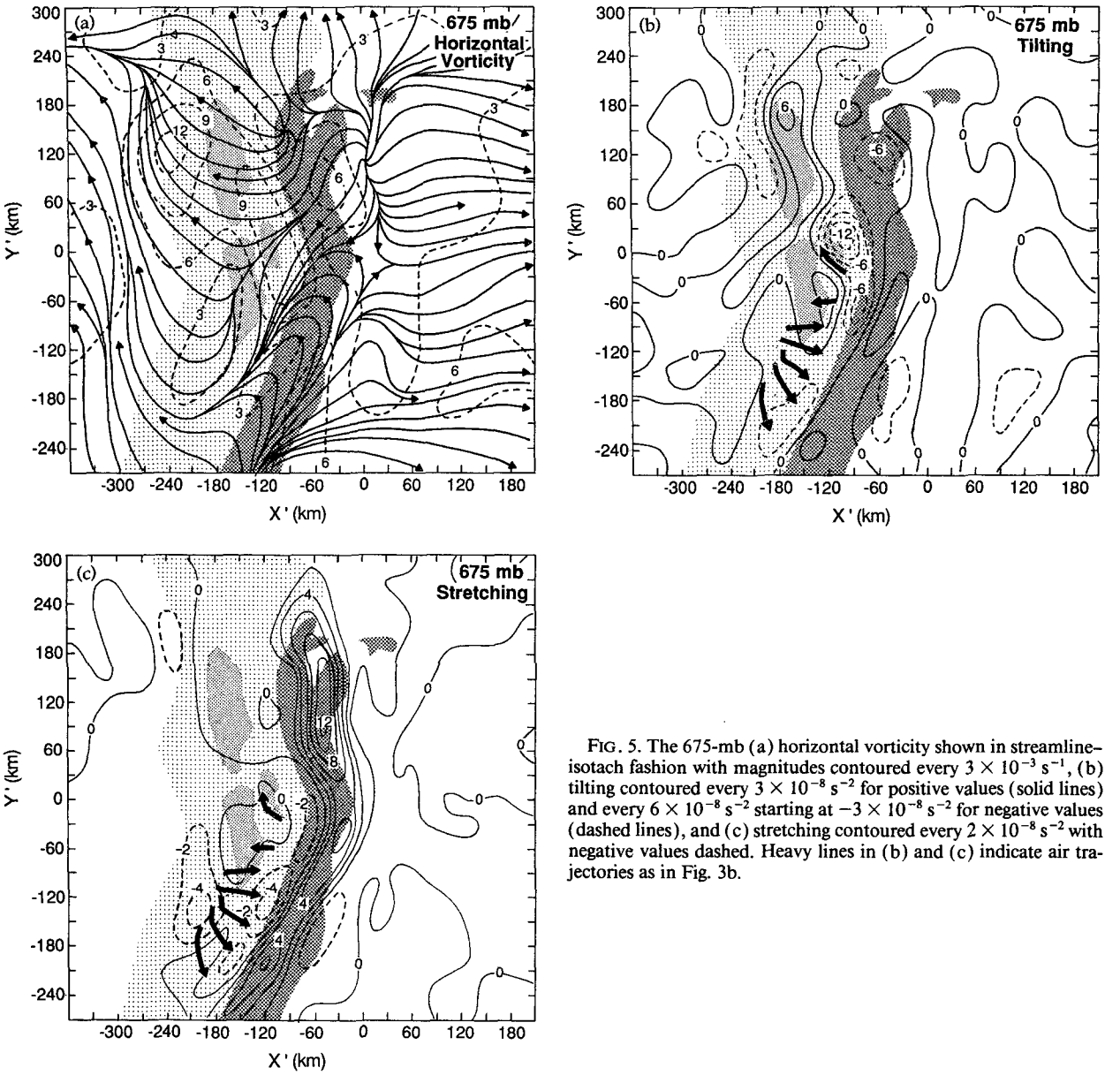

FIG. 5. The 675-mb (a) horizontal vorticity shown in streamline-isotach fashion with magnitudes contoured every 3×10^{-3} s^{-1}, (b) tilting contoured every 3×10^{-8} s^{-2} for positive values (solid lines) and every 6×10^{-8} s^{-2} starting at -3×10^{-8} s^{-2} for negative values (dashed lines), and (c) stretching contoured every 2×10^{-8} s^{-2} with negative values dashed. Heavy lines in (b) and (c) indicate air trajectories as in Fig. 3b.

of contour analysis (e.g., Figs. 5b and 5c). Since, mathematically, tilting is the dot product between the horizontal-vorticity vector and the gradient of vertical motion, the magnitude of tilting is maximized where the horizontal-vorticity vector lies parallel to the gradient of vertical motion.

b. The band of anticyclonic vorticity

Backward air trajectories were calculated from the band of anticyclonic vorticity observed at 675 mb to determine the effects of tilting and stretching on the vertical vorticity of the air as it flowed through that part of the storm. Uncertainties associated with the limited horizontal resolution of vertical motion in the southern portion of the squall-line system restricted the starting position of the trajectories to the rearward half of the band of anticyclonic vorticity. Closer to the convective region, the aliasing of upward motion associated with the convective line onto the surrounding area by the current analysis technique was evident (see Fig. 13d in BH) and would have resulted in rising, rather than sinking, air trajectories. Analysis of the Doppler radar data in the northern portion of the 10–11 June 1985 storm indicates that the air at midlevels between the heaviest stratiform precipitation and the rear of the convective line was generally subsiding (Rutledge et al. 1988a). Moreover, the band of anticyclonic vorticity observed at midlevels in the modeling study of ZGP was associated with subsidence. Given

that the horizontal gradients of vertical motion near the convective line in the 10–11 June 1985 storm were large (see Fig. 4 in Houze et al. 1989), the filter applied to the horizontal winds during the composite analysis apparently aliased the strong divergence associated with the convective line onto the surrounding area. Integrating the divergence to diagnose vertical motion then resulted in an overly broad region of upward motion near the convective line. To alleviate this aliasing effect, 0.5 Pa s^{-1} (i.e., about -6 cm s^{-1} at 675 mb) was added to the diagnosed vertical motions and the trajectories were terminated after 2 h or when upward motion in excess of 0.5 Pa s^{-1} was encountered. These measures were necessary to ensure that the trajectories were consistent with higher-resolution analyses and the modeling study of ZGP; all of which indicate sinking motion at midlevels between the heaviest stratiform precipitation and the rear of the convective line.

The trajectories, so determined (seen in Figs. 3b and 5), reveal that the subsiding air had traveled rear-to-front in moderate storm-relative flow, except near the central portion of the system where the relative flow was weak or slightly front to rear. Close inspection of the trajectories further reveal that the air took about 1 h to subside from 640 to 675 mb. Even without the addition of 0.5 Pa s^{-1} to the diagnosed vertical motions, the air subsided slowly as it approached 675 mb. Thus, the air was subject to tilting and stretching similar to the patterns observed at 675 mb (Fig. 5) for a relatively long period of time ($\sim$1 h).

At midlevels the horizontal vorticity vector was oriented generally across the storm system from front to rear (e.g., Fig. 5a) with a component parallel to the gradient of vertical motion (see Fig. 13d in BH). Consequently, as air parcels descended, their horizontal vorticity was tilted into anticyclonic vertical vorticity at rates typically -2 to -3×10^{-8} s^{-2} (Fig. 5b). Tilting thus favored the production of anticyclonic vorticity within the air parcel as it traveled through the region between the strong mesoscale downdraft associated with the heaviest stratiform precipitation and the region of weaker descent toward the convective line. Further concentration of anticyclonic vorticity was accomplished by stretching as the air was carried downwind (Fig. 5c). Tilting and stretching were of the same order of magnitude, but along most of the trajectory, tilting was dominant by a factor of 2–3. Combined, tilting and stretching led to the development of anticyclonic vorticity at rates near -6×10^{-8} s^{-2} throughout a significant portion of the stratiform region of the 10–11 June 1985 storm (i.e., between the heaviest stratiform precipitation and the rear of the convective line). In view of the 1-h period that the air was near 675 mb, the magnitude of tilting and stretching agrees well with the magnitudes of vertical vorticity observed in the anticyclonic vorticity band at 675 mb (Fig. 3b). Thus, the band of anticyclonic vorticity at 675 mb was evidently maintained by the tilting of horizontal vorticity with further concentration by stretching just downwind of the tilting.

An analogous series of events explains the observed anticyclonic vorticity above the melting level where, as exemplified by the 550-mb level (Fig. 3a), the band of anticyclonic vorticity (between $X' = -135$, -75 and $Y' = -30$, 180) was associated with tilting of horizontal vorticity by downward motion associated with the transition zone downdraft (BH) in the stratiform region immediately behind the convective line and by upward motion in the convective region. However, the gradients of vertical motion associated with the transition zone downdraft were much weaker than those associated with the upward motion in the convective line. Thus, above the melting level, the tilting of horizontal vorticity into anticyclonic vertical vorticity was primarily associated with gradients of upward motion in the convective region rather than gradients of downward motion in the stratiform region. This relationship is further elucidated by comparing the location of the axis of maximum negative tilting (along the back of the convective region in Fig. 6c) with the location of the axis of maximum upward motion (over the convective region in Fig. 6b). Although the air parcel had positive vertical vorticity, while in the convective region, the tilting between the mean convective updraft and the transition zone downdraft was sufficient to change the sign of the relative vertical vorticity of the parcel as it traveled past the rear of the convective line. Since the front-to-rear relative flow (Fig. 6a) behind the transition zone downdraft was ascending, anticyclonic vorticity was eventually carried upward and rearward. As indicated by the negative values of stretching at 550 mb (between $X' = -135$, -90 and $Y' = -30$, 165 in Fig. 6d), the stretching remained favorable for concentrating the anticyclonic vorticity as the air was carried up and back.

c. *The band of cyclonic vorticity*

The tilting and stretching mechanisms can also be used to interpret the band of cyclonic vorticity observed from 550 to 675 mb (Figs. 3a and 3b) along the back edge of the stratiform region. We focus on the cyclonic vorticity evident in the northern portion of the stratiform region at 550 mb (between $X' = -300$, -225 and $Y' = 60$, 270 in Fig. 3a). Backward trajectories using the unadjusted diagnosed vertical motions and observed relative flow indicate that this air had subsided from approximately 420 mb over roughly 2 h as it moved forward and northward relative to the storm. At 500 mb, the horizontal vorticity (Fig. 7a) in this region had a negative across-line component (i.e., the horizontal vorticity vectors were oriented somewhat across the storm from front to rear). Strong subsidence associated with dry rear-to-front flow was observed at the rear edge of the stratiform precipitation pattern

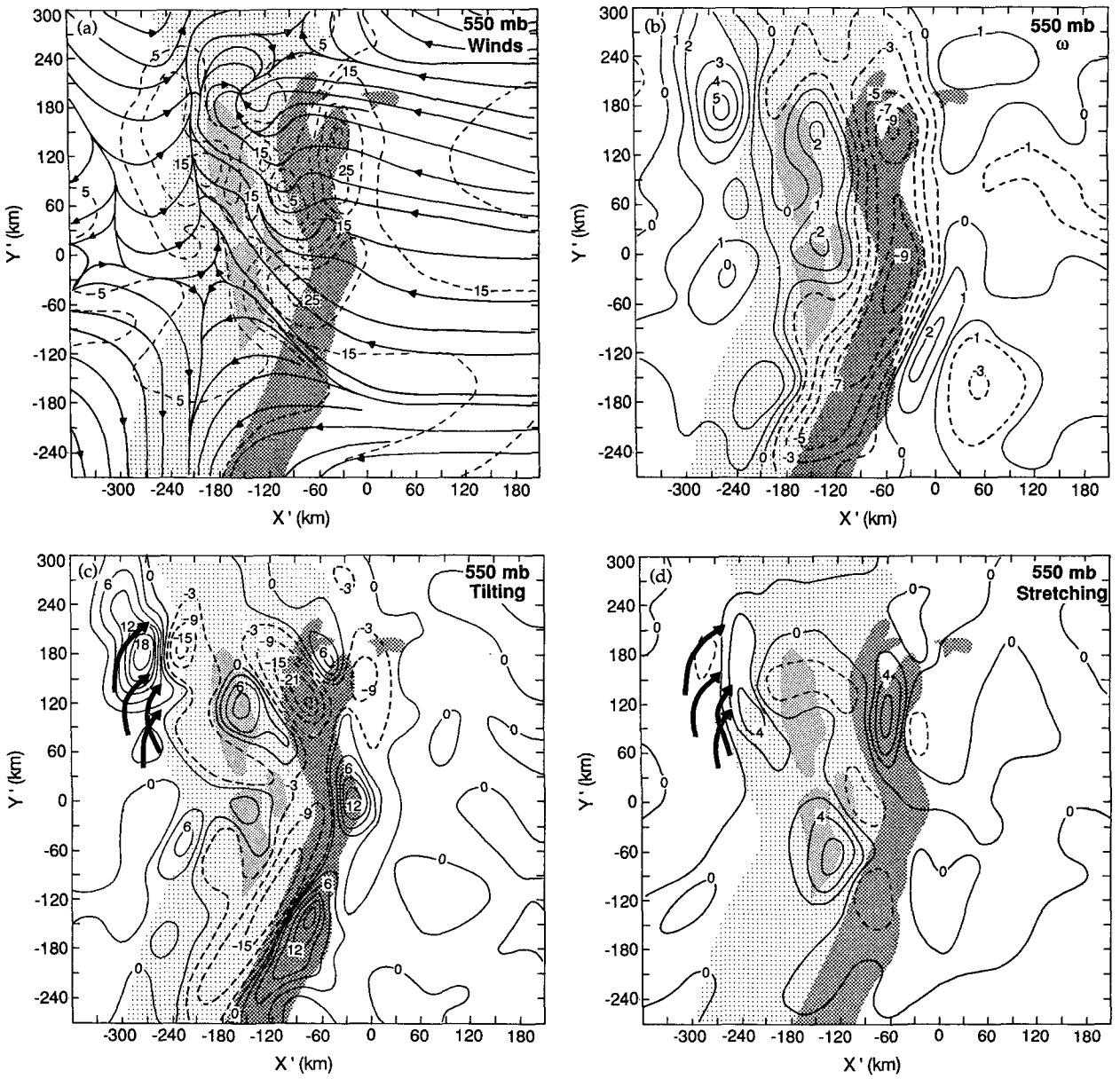

FIG. 6. The 550-mb (a) storm-relative flow with isotachs contoured every 5 m s^{-1}, (b) vertical motion contoured every 1 Pa s^{-1} for positive values (solid lines) and every 2 Pa s^{-1} for negative values (dashed lines), (c) tilting contoured every 3×10^{-8} s^{-2} for positive values (solid lines) and every 6×10^{-8} s^{-2} starting at -3×10^{-8} s^{-2} for negative values (dashed lines), and (d) stretching contoured every 2×10^{-8} s^{-2} with negative values dashed. Heavy lines in (c) and (d) indicate air trajectories as in Fig. 3a.

between 550 and 500 mb (Figs. 6a and 6b here and Figs. 12a and 12c in BH). Thus, a tilting couplet (centered at $X' = -270$, $Y' = 190$ in Fig. 7b) with cyclonic vertical vorticity produced to the rear of the maximum downward motion and anticyclonic vorticity produced ahead of the maximum downward motion was located along the back edge of the stratiform region where the gradient of vertical motion changed signs. As rear-to-front relative flow (Fig. 6a here and Fig. 12a in BH) transported the air within the cyclonic part of the tilting couplet forward, stretching (although small compared to tilting) associated with convergence in the rear-to-front flow continued to concentrate the cyclonic vorticity (between $X' = -300$, -255 and $Y' = 60$, 240 at 500 mb in Fig. 7c, and between $X' = -270$, -210 and $Y' = 60$, 240 at 550 mb in Fig. 6d). Thus, it appears that this band of vertical vorticity was maintained by the same series of processes as the anticyclonic vorticity band farther ahead: tilting of horizontal vorticity by horizontal gradients of vertical motion, with further concentration by stretching as the relative flow carried the air downwind.

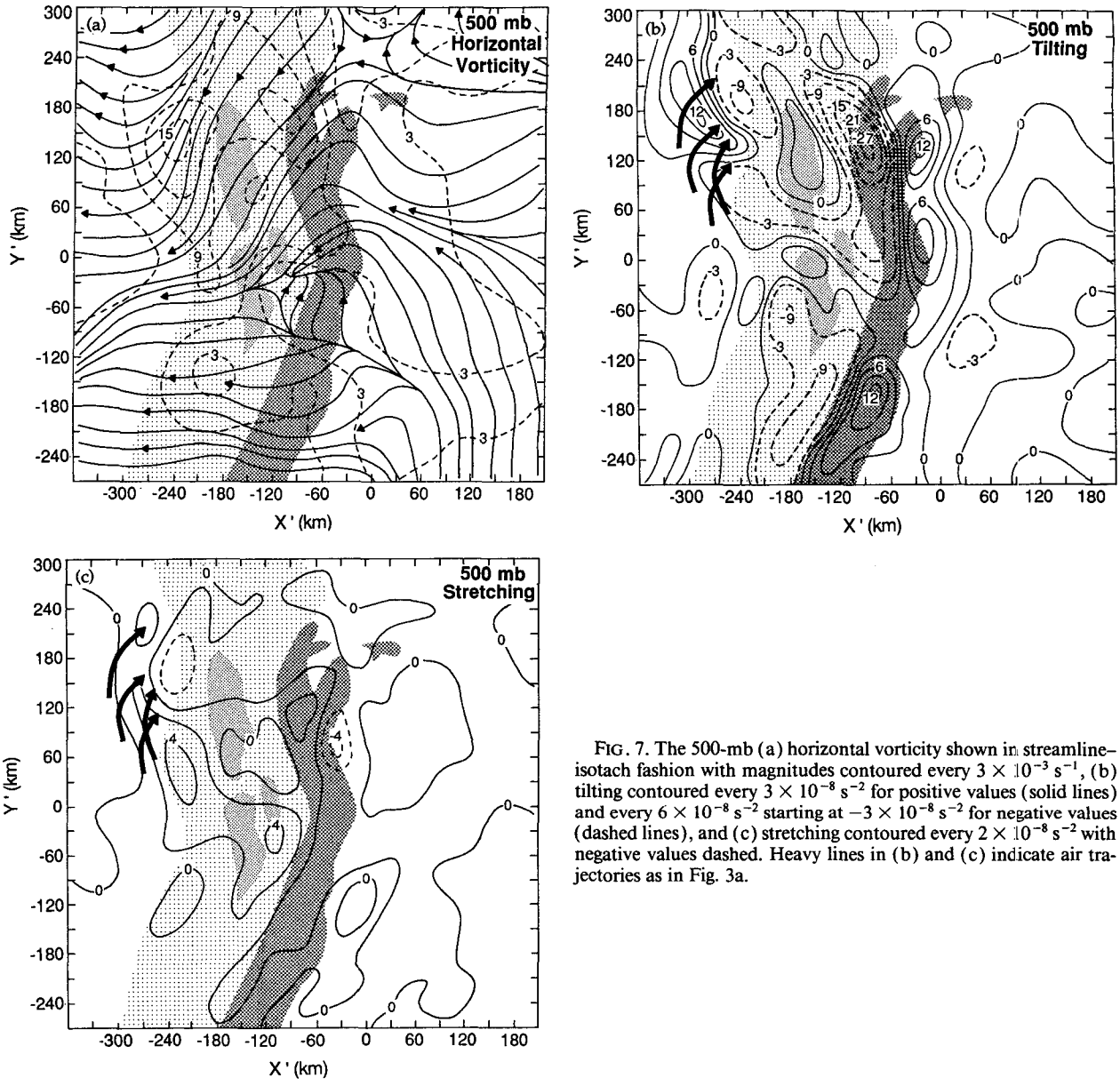

FIG. 7. The 500-mb (a) horizontal vorticity shown in streamline–isotach fashion with magnitudes contoured every 3×10^{-3} s^{-1}, (b) tilting contoured every 3×10^{-8} s^{-2} for positive values (solid lines) and every 6×10^{-8} s^{-2} starting at -3×10^{-8} s^{-2} for negative values (dashed lines), and (c) stretching contoured every 2×10^{-8} s^{-2} with negative values dashed. Heavy lines in (b) and (c) indicate air trajectories as in Fig. 3a.

It should be noted that the band of cyclonic vorticity that has been examined is not directly associated with the deep mesovortex discussed by ZGP in the numerical simulation of this storm system. In particular, their Figure 28b shows that a cyclonic circulation was present at roughly 850 mb to the north of the genesis region well before the squall-line system developed. That circulation apparently interacted with the convective storm and formed a deep mesolow and associated mesovortex. However, as is evident from their Fig. 31, the deep mesovortex was located in the northern portion of the *convective* region (see also their Fig. 19). The *analysis* of this storm system also shows a deep, strong mesolow with an associated region of strong positive vorticity in the northern portion of the convective region (see Figs. 3a–3c here and Figs. 13a and 13e; 14a and 14b; and 15b in BH). Positive vorticity *in the trailing stratiform region* at midlevels was weaker than the mesovortex in the convective region in both the simulation of ZGP and in the analysis presented here. Since this analysis assumes a steady state, the development of the vorticity in the convective region cannot be addressed.

5. Discussion

The banded midlevel vorticity structure of the stratiform region of the 10–11 June 1985 squall line was

primarily maintained by tilting of horizontal vorticity by nonuniform vertical motions associated with the squall-line system. Stretching further concentrated the vorticity but was less than the effect of tilting by a factor of 2–10. In the cases of the anticyclonic vorticity observed below the melting level between the heaviest stratiform precipitation and the convective line, and the cyclonic vorticity observed near the back edge of the stratiform region at 550 mb, the tilting was produced by gradients of subsidence within the stratiform region.

Verlinde and Cotton (1990) recently observed a meso-β-scale vortex couplet near the convective region of a weak multicellular convective complex and showed that the mesovortices resulted from the vertical transport of low-level momentum by an ensemble of convective updrafts rather than by tilting of horizontal vorticity by vertical motions within the stratiform region. Consistent with the difference in mechanisms between the two storm systems, the circulations associated with the vortex couplet observed by Verlinde and Cotton were quite deep (extending from 3 to 11 km) and small in radius ($\sim$15 km) compared to the banded vortex pattern observed in the 10–11 June 1985 squall line that was relatively shallow (2–6 km) but quite large in horizontal scale ($\sim$100 km).

Brandes (1990) noted that tilting of horizontal vorticity by gradients of vertical motion within the stratiform region may have helped the low-level development of a cyclonic mesovortex observed near the rear of the trailing stratiform region of the 6–7 May 1985 squall-line system. The cyclonic circulation that he observed was comparable in depth and horizontal scale to the cyclonic vorticity observed in the 10–11 June 1985 storm. In the 6–7 May 1985 storm, however, the cyclonic circulation apparently dominated the stratiform precipitation region, but in the 10–11 June 1985 storm, the cyclonic circulation was just one small perturbation on the broader-scale rear-to-front flow (see Fig. 13a in BH). Consistent with the difference in influence of the cyclonic circulations on the observed storm structures, the 6–7 May 1985 case had an asymmetric stratiform precipitation structure (i.e., stratiform rain confined mainly to the northern portion of the squall-line system where the front-to-rear branch of the cyclonic vortex resided), while the 10–11 June 1985 storm had stratiform precipitation distributed almost uniformly behind the convective line.

The differences in symmetry of the stratiform regions of the 6–7 May 1985 and 10–11 June 1985 cases may have been associated with differences in the development of the midlevel vertical vorticity in those two storms. For instance, Brandes suggests that the horizontal vorticity that was tilted into vertical vorticity at low levels may have originated from horizontal buoyancy gradients across the cyclonic vortex, which had low temperatures associated with the heavy stratiform precipitation in the front-to-rear branch and high temperatures associated with the weak stratiform precipitation in the rear inflow branch of the mesovortex at 3 km. Since the stratiform precipitation was more uniform in the 10–11 June 1985 storm, the production of horizontal vorticity by buoyancy gradients might have been less important. Additionally, Brandes (1990) showed that at midlevels the amplification of vertical vorticity by stretching was primarily associated with convergence in the rear-inflow branch of the vortex. Since the rear inflow in the 6–7 May 1985 storm was not as broad as in the 10–11 June 1985 storm, the stretching was more localized and could have spun the circulation into a well-defined vortex instead of an elongated band of cyclonic vorticity, like that observed in the 10–11 June 1985 storm.

In numerical simulations of mesoscale convective systems (MCSs), Zhang and Fritsch (1987, 1988a,b) showed that inertially stable cyclonic mesovortices can develop from geostrophic adjustment in response to a mesolow that typically forms beneath the warm trailing anvil cloud. A trough and mesolow were observed in association with the band of cyclonic vorticity near the rear of the stratiform precipitation region of the 10–11 June 1985 storm (see Fig. 13e in BH). However, as evidenced by the cross-gradient flow at 675 mb (compare Figs. 13a and 13e in BH), the winds in the 10–11 June 1985 storm were not balanced. Moreover, the 10–11 June 1985 storm exhibited an equally large area of anticyclonic vorticity that formed between the rear of the convective line and the heaviest stratiform precipitation.

This band of anticyclonic vorticity was also observed in a simulation of the 10–11 June 1985 storm (ZGP), but no indication was given concerning the role of this feature on the internal dynamics of the storm system. It has been speculated that the midlevel anticyclonic vorticity may have been detrimental to the longevity of the storm system by inhibiting the development of an inertially stable cyclonic circulation. Further examination of the tilting process by which the band of anticyclonic vorticity was maintained and may have been developed reveals that the tilting was of horizontal vorticity vectors with a negative across-line component (i.e., oriented with a component perpendicular to the convective line from front to rear). Since, in the stratiform region, horizontal vorticity was primarily associated with vertical shear of the horizontal wind,

$$\omega_H \approx -\frac{\partial v}{\partial z}\,\mathbf{i} + \frac{\partial u}{\partial z}\,\mathbf{j}, \tag{4}$$

a negative component of across-line horizontal vorticity implies a positive vertical shear of the along-line wind component ($\partial v/\partial z > 0$). The 10–11 June 1985 storm exhibited strong shear in the along-line wind component in both the environment ahead of the storm and in the stratiform precipitation region. Although examination of how this shear developed is beyond the

scope of the current research, it is interesting to note that such a shear profile is characteristic of an environment just ahead of a cold front and that the 10–11 June 1985 storm apparently developed just ahead of a weak cold front (Johnson and Hamilton 1988; ZGP). Thus, large-scale baroclinity may have established a horizontal vorticity field that, when acted upon by the mesoscale vertical motions within the storm system, produced bands of vertical vorticity orientated parallel to the convective line.

Complicating this argument, however, is the fact that the across-line horizontal vorticity of the air within the 10–11 June 1985 storm may have been affected by generation through horizontal buoyancy gradients and by tilting of other vorticity components into the across-line direction. Since the trailing stratiform precipitation was almost uniformly distributed along the squall-line system, the generation of across-line horizontal vorticity by along-line buoyancy gradients would likely have been small. Moreover, the airflow in the banded vorticity structures discussed above was primarily rear to front and may have retained some of the characteristics of the horizontal vorticity associated with the environment behind the squall-line system. However, tilting of other vorticity components into across-line horizontal vorticity was active. In particular, analyses at 500 and 550 mb indicate that near the back edge of the stratiform region along-line horizontal vorticity (which would have been affected by across-line buoyancy gradients between the clear and cloudy air and differential cooling across the light and heavy stratiform precipitation regions) was tilted (horizontally) into negative across-line horizontal vorticity by along-line gradients in the rear inflow, which, at those levels, was strongest in the northern portion of the squall-line system (see Fig. 6a here and Fig. 12a in BH). Moreover, the analyses also indicated that tilting of absolute vertical vorticity by the vertical shear of the across-line wind further contributed to the negative across-line horizontal vorticity near the back edge of the stratiform region. Consequently, without further information on the evolution of the squall-line system and its environment, it is not possible to determine if the negative across-line horizontal vorticity (which was acted upon by the mesoscale vertical motions within the storm system to maintain and possibly produce the bands of positive and negative vertical vorticity at midlevels in the stratiform region) was associated with shear in the large-scale baroclinic environment or with circulations that developed in response to the storm system itself.

6. Conclusions

The comprehensive composite analysis of BH in which high-frequency rawinsonde, profiler, and surface mesonet data were combined with dual-Doppler analyses in a common framework attached to the moving storm has allowed us to examine the midlevel vertical-vorticity structure of the mature squall-line system. Figure 8a is a conceptual model showing the distribution of vertical vorticity in a cross section normal to the convective line of the 10–11 June 1985 storm. Strong positive vorticity was evident throughout the depth of the convective region and at mid-to-low levels in the rearward half of the trailing stratiform region with the maximum cyclonic vorticity (labeled *P*) observed near the radar bright band, associated with the melting level, just behind the heaviest stratiform precipitation. Anticyclonic vorticity was observed between the two regions of cyclonic vorticity. The maximum anticyclonic vorticity (labeled *N*) was also observed near the melting level (i.e., the radar bright band) but closer to the convective line. Thus, from approximately 500 to 800 mb, bands of positive and negative vertical vorticity, oriented parallel to the convective line, were found over most of the stratiform region with negative vorticity between the rear of the convective line and the area of heaviest stratiform precipitation and positive vorticity farther back. This pattern of banded vertical vorticity also appeared in a numerical simulation of the 10–11 June 1985 storm (ZGP). Although close examination of previous *observational* studies of squall lines similar to the 10–11 June 1985 storm indicates that concentrations of positive vorticity at midlevels are typically found just behind (not collocated with) the heaviest stratiform precipitation, sufficiently detailed wind data over a broad-enough region were not available to determine whether a band of anticyclonic vorticity at midlevels between the convective line and the cyclonic vorticity was also present.

Since the banded midlevel vertical-vorticity structure of the stratiform region of the 10–11 June 1985 squall-line system is a newly observed feature, we used the composite analysis of BH to compute the tilting and stretching terms of the vertical-vorticity equation and relevant air trajectories to determine how the vertical vorticity of the air may have changed as it flowed through the storm system. Based on this information, a conceptual model summarizing how the vertical-vorticity pattern (Fig. 8a) was maintained and may have developed is shown in Fig. 8b. In particular, we focus on the maximum and minimum vertical vorticity (indicated by *P* and *N*, respectively, in Fig. 8b) observed near the melting level and on the anticyclonic vorticity observed above the melting level in the stratiform region.

Possibly related to large-scale baroclinity in which the 10–11 June 1985 storm formed, vertical shear of the along-line wind component resulted in horizontal vorticity (represented in Fig. 8b by vortex "tubes") oriented perpendicular to the convective line across the storm system from front to rear. Tilting of the horizontal vorticity by gradients of subsidence associated with the dry rear inflow (labeled "rear-inflow subsidence" in Fig. 8b) at the back of the stratiform region produced a couplet of positive and negative vertical-

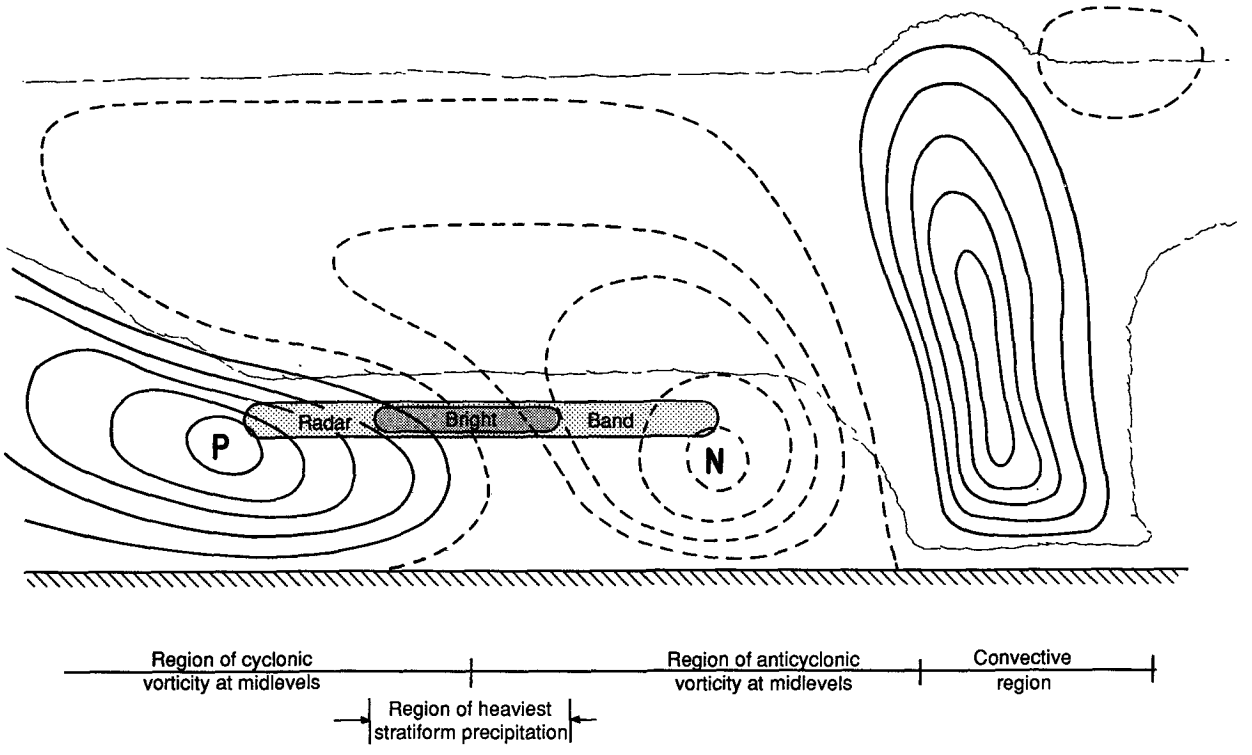

(a)

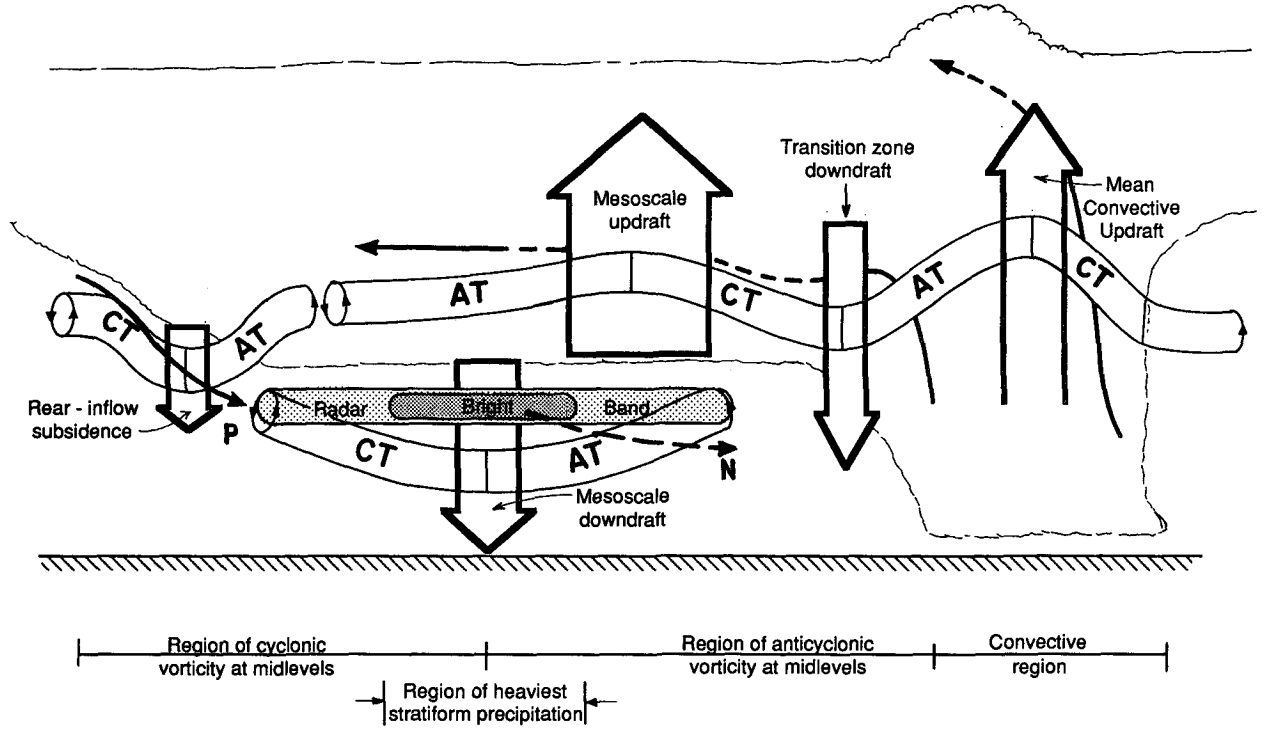

(b)

FIG. 8. Conceptual model for (a) the distribution of relative vertical vorticity in a cross section taken normal to the convective line of the 10–11 June 1985 storm with solid (dashed) lines indicating positive (negative) vorticity and contours in the convective region at twice the interval used in the stratiform region, and (b) the tilting and stretching necessary to explain the observed vertical-vorticity pattern shown in (a) for the 10–11 June 1985 squall-line system.

vorticity changes (labeled CT and AT, respectively, in Fig. 8b). Air trajectories (illustrated in Fig. 8b by thin arrows) computed backward from the maximum positive vertical vorticity (P) observed at midlevels near the rear of the heaviest stratiform precipitation suggested that this air had subsided through the CT part of the tilting couplet. As indicated by the solid (rather than dashed) segment of the air trajectory, stretching favored the concentration of positive vorticity as the air was carried forward and downward to the region of maximum cyclonic vorticity (i.e., to P in Fig. 8b). Even though weak tilting favored the further development of cyclonic vorticity beyond P, the vertical vorticity of the air would have been decreased by the strong divergence observed at levels below the radar bright band (BH).

The anticyclonic vorticity observed at midlevels between the convective region and the heaviest stratiform precipitation was also accounted for by the effects of tilting and stretching. Here the tilting was associated with gradients of subsidence in the mesoscale downdraft. Air trajectories computed backward from the center of the negative vorticity band (N) suggested that this air had subsided slowly in weak relative flow near the melting level. The weak relative flow assured that tilting would affect the vertical vorticity of the air for a long period of time, eventually causing the absolute vertical vorticity to become negative. Thereafter, as indicated by the dashed segments of the air trajectory, stretching was able to further concentrate anticyclonic vorticity as the air flowed slowly downwind.

Above the melting level (i.e., above the radar bright band in Fig. 8b), the anticyclonic vorticity was maintained mainly by strong tilting associated with gradients of vertical motion between the mean convective updraft and the weaker transition zone downdraft. As air flowed through this region of strong tilting, the absolute vorticity quickly became negative so that stretching further concentrated anticyclonic vorticity. Despite weak cyclonic tilting associated with gradients of vertical motion in the mesoscale updraft to the rear of the transition zone downdraft, the absolute vorticity of the air remained negative as it was carried rearward and upward. Since stretching, associated with convergence, acted opposite to the tilting, there was little change in the vertical vorticity of the air as it flowed through this part of the storm. Analyses of tilting and stretching at upper levels (not shown) indicate that divergent airflow acted to decrease the relative anticyclonic vorticity of the air as it was carried farther aloft. However, the decrease in anticyclonic vorticity was partially offset by weak anticyclonic tilting associated with gradients of vertical motion in the mesoscale updraft to the rear of the updraft maximum.

Assuming that the physical processes that maintained the observed vertical-vorticity structure were also the processes that formed it, the combined magnitudes of tilting and stretching were sufficient to have formed the observed midlevel banded vertical-vorticity structure (Fig. 8a) in about 1–2 h. Tilting, which is a factor of 2–10 greater than stretching, was the dominant term. Stretching acted only to amplify the resulting absolute vorticity of the air. Thus, the band of anticyclonic vorticity observed at midlevels between the rear of the convective region and the heaviest stratiform precipitation could not have been maintained without the strong anticyclonic tilting observed in the stratiform region of the 10–11 June 1985 storm.

The midlevel band of anticyclonic vorticity may have negatively affected the longevity of the storm system. Since the anticyclonic vorticity of the air over much of the stratiform region was greater in magnitude than the local Coriolis parameter, the air had negative absolute vorticity that is associated with inertial instability. Consequently, the development of an inertially stable circulation, thought to be characteristic of long-lived storm systems, would have been impaired by the concentration of anticyclonic vorticity in the stratiform region of the 10–11 June 1985 storm. Consistent with the lack of an inertially stable cyclonic mesovortex, the 10–11 June 1985 storm was not particularly long lived.

Acknowledgments. Dr. D. D. Churchill provided valuable support in developing software for this study. G. C. Gudmundson edited the manuscript and K. M. Dewar drafted the figures. This research was funded by the National Science Foundation under Grant ATM-8719838.

REFERENCES

Biggerstaff, M. I., and R. A. Houze, Jr., 1991: Kinematic and precipitation structure of the 10–11 June 1985 squall line. *Mon. Wea. Rev.*, **119**, 3034–3065.

Brandes, E. A., 1990: Evolution and structure of the 6–7 May 1985 mesoscale convective system and associated vortex. *Mon. Wea. Rev.*, **118**, 109–127.

Chong, M., P. Amayenc, G. Scialom and J. Testud, 1987: A tropical squall line observed during the COPT 81 experiment in West Africa. Part I: Kinematic structure inferred from dual-Doppler radar data. *Mon. Wea. Rev.*, **115**, 670–694.

Cunning, J. B., 1986: The Oklahoma–Kansas Preliminary Regional Experiment for STORM-Central. *Bull. Amer. Meteor. Soc.*, **67**, 1478–1486.

Gamache, J. F., and R. A. Houze, Jr., 1982: Mesoscale air motions associated with a tropical squall line. *Mon. Wea. Rev.*, **110**, 118–135.

——, and ——, 1985: Further analysis of the composite wind and thermodynamic structure of the 12 September GATE squall line. *Mon. Wea. Rev.*, **113**, 1241–1259.

Holton, J. R., 1979: *An Introduction to Dynamic Meteorology.* Academic Press, 391 pp.

Heymsfield, G. M., and S. Schotz, 1985: Structure and evolution of a severe squall line over Oklahoma. *Mon. Wea. Rev.*, **113**, 1563–1589.

Houze, R. A., Jr., 1977: Structure and dynamics of a tropical squall-line system. *Mon. Wea. Rev.*, **105**, 1540–1567.

——, S. A. Rutledge, M. I. Biggerstaff and B. F. Smull, 1989: Interpretation of Doppler weather-radar displays of midlatitude mesoscale convective systems. *Bull. Amer. Meteor. Soc.*, **70**, 608–619.

Johnson, R. H., and P. J. Hamilton, 1988: The relationship of surface-pressure features to the precipitation and air-flow structure of an intense midlatitude squall line. *Mon. Wea. Rev.*, **116,** 1444–1472.

Kessinger, C. J., P. S. Ray and C. E. Hane, 1987: The Oklahoma squall line of 19 May 1977. Part I: A multiple Doppler analysis of convective and stratiform structure. *J. Atmos. Sci.*, **44,** 2840–2864.

Leary, C. A., and E. N. Rappaport, 1987: The life cycle and internal structure of a mesoscale convective complex. *Mon. Wea. Rev.*, **115,** 1503–1527.

Ogura, Y., and M. T. Liou, 1980: The structure of a midlatitude squall line. *J. Atmos. Sci.*, **37,** 553–567.

Orlanski, I., 1975: A rational subdivision of scales for atmospheric processes. *Bull. Amer. Meteor. Soc.*, **56,** 527–530.

Roux, F., 1988: The West African squall line observed on 23 June 1981 during COPT 81: Kinematics and thermodynamics of the convective region. *J. Atmos. Sci.*, **45,** 406–426.

Rutledge, S. A., R. A. Houze, Jr., M. I. Biggerstaff and T. Matejka, 1988a: The Oklahoma–Kansas mesoscale convective system of 10–11 June 1985: Precipitation structure and single-Doppler radar analysis. *Mon. Wea. Rev.*, **116,** 1409–1430.

Smull, B. F., and R. A. Houze, Jr., 1987: Dual-Doppler radar analysis of a midlatitude squall line with a trailing region of stratiform rain. *J. Atmos. Sci.*, **44,** 2128–2148.

Srivastava, R. C., T. J. Matejka and T. J. Lorello, 1986: Doppler-radar study of the trailing-anvil region associated with a squall line. *J. Atmos. Sci.*, **43,** 356–377.

Verlinde, J., and W. R. Cotton, 1990: A mesoscale vortex couplet observed in the trailing anvil of a multicellular convective complex. *Mon. Wea. Rev.*, **118,** 993–1010.

Zhang, D.-L., and J. M. Fritsch, 1987: Numerical simulation of the meso-β scale structure and evolution of the 1977 Johnstown flood. Part II: Inertially stable warm-core vortex and the mesoscale convective complex. *J. Atmos. Sci.*, **44,** 2593–2612.

——, and ——, 1988a: Numerical sensitivity experiments of varying model physics on the structure, evolution, and dynamics of two mesoscale convective systems. *J. Atmos. Sci.*, **45,** 261–293.

——, and ——, 1988b: A numerical investigation of a convectively generated, inertially stable, extratropical, warm-core mesovortex over land. Part I: Structure and evolution. *Mon. Wea. Rev.*, **116,** 2660–2687.

——, K. Gao and D. B. Parsons, 1989: Numerical simulation of an intense squall line during 10–11 June 1985 PRE-STORM. Part I: Model verification. *Mon. Wea. Rev.*, **117,** 960–994.